Pressure dependence of the electronic structure and spin state in $Fe_{1.01}Se$ superconductors probed by x-ray absorption and x-ray emission spectroscopy

J. M. Chen,[1,*] S. C. Haw,[1] J. M. Lee,[1,3] T. L. Chou,[1] S. A. Chen,[1] K. T. Lu,[1] Y. C. Liang,[1] Y. C. Lee,[1] N. Hiraoka,[1] H. Ishii,[1] K. D. Tsuei,[1] Eugene Huang,[2] and T. J. Yang[3]

[1]*National Synchrotron Radiation Research Center (NSRRC), Hsinchu, Taiwan, Republic of China*

[2]*Center for General Education, Chung Chou Institute of Technology, Changhua County, Taiwan, Republic of China*

[3]*Department of Electrophysics, National Chiao Tung University, Hsinchu, Taiwan, Republic of China*

(Received 25 April 2011; revised manuscript received 4 July 2011; published 9 September 2011)

Pressure dependence of electronic structures and spin states of iron-chalcogenide $Fe_{1.01}Se$ superconductors up to ~66 GPa has been investigated with x-ray emission spectra and x-ray absorption spectra with partial-fluorescence yield. The intensity of the pre-edge peak at energy of ~7112.7 eV of the Fe *K*-edge x-ray absorption spectrum of $Fe_{1.01}Se$ decreases progressively with pressure up to ~10 GPa. A new prepeak at energy of ~7113.7 eV develops for pressure above ~13 GPa, indicating formation of a new phase. The experimental and the calculated Fe *K*-edge absorption spectra of $Fe_{1.01}Se$ using the FDMNES code agree satisfactorily. The larger compression accompanied by significant distortion around the Fe atoms along the *c* axis in $Fe_{1.01}Se$ upon applying pressure suppresses the Fe 3*d*-Se 4*p* and Fe 4*p*-Se 4*d* hybridization. The applied pressure suppresses the nearest-neighbor ferromagnetic superexchange interaction and enhances spin fluctuations on the Fe sites in $Fe_{1.01}Se$. A discontinuous variation of the integrated absolute difference values of the $K\beta$ emission line was observed, originating from a phase transition of $Fe_{1.01}Se$ for a pressure >12 GPa. $Fe_{1.01}Se$ shows a small net magnetic moment of Fe^{2+} at ambient pressure, probably arising from strong Fe-Fe spin fluctuations. The satellite line $K\beta'$ was reduced in intensity upon applying pressure and became absent for pressure >52 GPa, indicating a continuous reduction of the spin moment of Fe in $Fe_{1.01}Se$ superconductors. The experimental results provide insight into the spin state of $Fe_{1.01}Se$ superconductors under pressure.

DOI: 10.1103/PhysRevB.84.125117 PACS number(s): 74.25.Jb, 78.70.Dm, 78.70.En

I. INTRODUCTION

The discovery of unconventional high-T_c superconductors in iron-based oxypnictide compounds $LaFeAsO_{1-x}F_x$ with a T_c of ~26 K has sparked interest in layered FeAs systems.[1,2] Other compounds belonging to the same family, $LnFeAsO_{1-x}F_x$ (Ln = Ce, Pr, Nd, Sm), with $T_c \leqslant$ ~55 K in $SmFeAsO_{1-x}F_x$ are known.[3–5] A new superconductor in an arsenic-free PbO-type β-$FeSe_x$ compound with a T_c of ~8 K was reported.[6] A large enhancement of T_c was observed in a tetragonal $Fe_{1.01}Se$ superconductor under pressure.

T_c of $Fe_{1.01}Se$ increased to as much as 27 K on applying pressure (P) $\leqslant$ 1.5 GPa and then increased to 34–37 K with pressure from 8.9 to 22 GPa.[7–11] This PbO-type β-$FeSe_x$ compound is a candidate for industrial applications, such as superconducting metal-sheathed wires.[12] At ambient pressure and room temperature, $Fe_{1.01}Se$ has a tetragonal PbO-type structure of ($P4/nmm$) composed of a stack of edge-sharing $FeSe_4$-tetrahedra layer by layer along the *c* axis.[6] The $Fe_{1.01}Se$ compound exhibits planar FeSe layers similar to FeAs layers in the FeAs-pnictide superconductors. X-ray diffraction (XRD) of $Fe_{1.01}Se$ at varied pressure by Medvedev *et al.*, show that at P < 12 GPa the tetragonal form dominates but at P > 12 GPa the sample contains a mixture of tetragonal and hexagonal (NiAs-type) ($P63/mmc$) forms.[8] A wide region of hexagonal and tetragonal phases is proposed, extending from $P \approx$ 7–35 GPa. Above 38 GPa, $Fe_{1.01}Se$ transforms to a hexagonal close-packed NiAs-type structure.[8] In contrast, a phase transition from the tetragonal to an orthorhombic symmetry ($Pbnm$) > 12 GPa and no mixed-phase region from 11 to 33 GPa was reported by several authors.[9,10,13] These results seem inconsistent. The local structure around Fe atoms and interlayer separation in Fe-based superconductors, including iron arsenides and chalcogenide, is correlated with T_c variation.[14] Further experimental investigation to provide direct information on the local structure around the Fe atoms in $Fe_{1.01}Se$ under pressure is accordingly indispensable.

The electronic states near the Fermi level in FeSe chalcogenide and FeAs pnictide are given by the Fe 3*d* orbitals and Se/As 4*p* orbitals.[15–17] The interaction of Fe 3*d* orbitals with the neighboring Se/As orbitals in the Fe-based superconductors affects their fundamental transport properties and physical nature.[18–21] Short-range antiferromagnetic (AFM) spin fluctuations for $Fe_{1.01}Se$, which were strongly enhanced toward T_c, were observed with ^{77}Se nuclear magnetic resonance (NMR) spectra.[22] The AFM spin fluctuation hence plays an important role in Fe-based superconductors.[15,16,22,23] Because interlayer Se-Se interactions of $Fe_{1.01}Se$ are weak, the application of external pressure has a profound influence on the local distortion around the Fe atoms and the hybridization between Fe 3*d* and interacting Se orbitals. Authors have proposed that superconductivity in $Fe_{1.01}Se$ is likely the result of an intricate interplay among their structural, magnetic, and electronic properties.[19,24] A comprehensive understanding of the evolution of magnetic spin states and the hybridization of the Fe 3*d* and the neighboring Se orbitals in $Fe_{1.01}Se$ with pressure is thus of key importance for the elucidation of superconducting properties of Fe-based materials.[25] However, detailed information about the pressure dependence of electronic structures and spin states of $Fe_{1.01}Se$ is sparse.

In addition to being sensitive to variation of electronic structure, x-ray absorption spectroscopy (XAS) with chemical selectivity is widely applied to provide insight complementary

to XRD measurements in the determination of the local environment around photoabsorber atoms.[26,27] We measured x-ray absorption spectra with partial fluorescence yield to obtain a high-resolution spectrum.[28] Fe K-edge x-ray absorption spectra at high resolution, particularly in the pre-edge region, provide accurate information about the electronic and local structure of $Fe_{1.01}Se$ under pressure. X-ray emission spectroscopy (XES) is directly sensitive to the magnetic structure of transition metals in materials and can probe the evolution of the spin state of the metal ion as a function of pressure.[29] In this work, we investigated the electronic structure, spin state, and structural transformation of iron-chalcogenide $Fe_{1.01}Se$ superconductors under $P \leqslant \sim 66$ GPa on recording lifetime-broadening-suppressed x-ray absorption spectra and x-ray emission spectra.

II. EXPERIMENTS

Polycrystalline samples of $Fe_{1.01}Se$ ($FeSe_{0.99}$) were synthesized from Fe 4N and Se 4N as initial materials in a stoichiometric molar ratio 1:0.99 by a solid-state reaction.[13] The reactants were weighed, mixed, ground, and pelletized in a glove box (Braun) under a purified argon atmosphere. The pellet was packed and sealed under a vacuum of $<10^{-4}$ Torr in a quartz tube and then calcined at 670 °C for 37 hr with intermediate grindings before quenching into a brine. The sample was characterized by refining the XRD pattern collected at the BL01C beamline at the National Synchrotron Radiation Research Center (NSRRC) using the Rietveld method. The $Fe_{1.01}Se$ sample contained a minor hexagonal $P63/mmc$ phase of the NiAs type, as reported elsewhere.[7–10,13] The PbO-type tetragonal phase of $Fe_{1.01}Se$ with a T_c of ~8 K is dominant. The molar fractions of the major tetragonal phase and the secondary hexagonal phase based on Rietveld refinements are 0.89 and 0.11, respectively.

A sample of $Fe_{1.01}Se$ as a finely grained powder was loaded into a hole (diameter 100 μm) of a Be gasket mounted on a Mao-Bell type diamond anvil cell (culet size 250 μm). Silicone oil served as a medium to transmit pressure. The pressure in the cell was measured through the line shift of ruby luminescence with an accuracy of ~0.1 GPa. The applied pressure was averaged at multiple points of the ruby luminescence before and after each spectral collection. All measurements were performed at room temperature.

Fe K-edge x-ray absorption and Fe $K\beta$ x-ray emission were measured at the Taiwan inelastic x-ray scattering beamline BL12XU at SPring-8. The undulator beam was made monochromatic with two Si(111) crystals and focused to a spot of area of $\sim 30 \times 30$ μm^2 at the sample position using two Kilpatrick-Baez focusing mirrors (length 1 m). The emitted x-ray fluorescence was collected at 90° from the incident x rays and analyzed with a Johann-type spectrometer equipped with a spherically bent Si(531) crystal (radius 1 m) and a solid-state detector arranged on a horizontal plane in the Rowland-circle geometry. The overall energy resolution, evaluated from the quasielastic scattering from the sample, had a full width of ~0.9 eV at half maximum about the emitted photon energy of 7058 eV. The Fe K-edge energies were calibrated by measuring a simultaneous standard of Fe metal foil with the known Fe K-edge absorption inflection point at 7112 eV and have an accuracy better than 0.05 eV. All absorption spectra are normalized to the incident beam intensity.

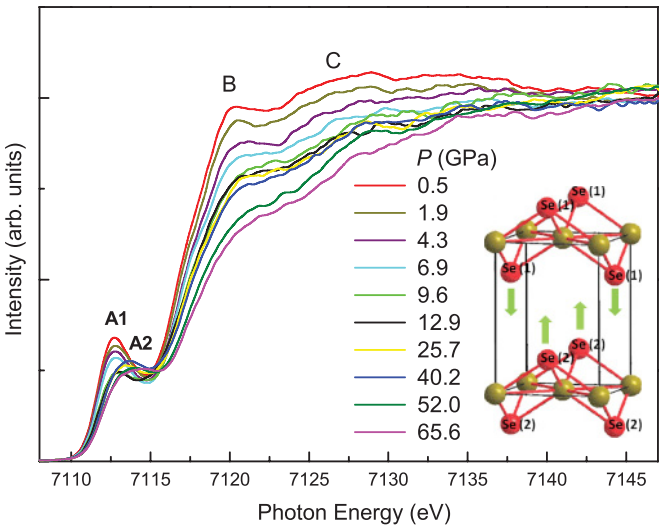

FIG. 1. (Color online) Fe K-edge x-ray absorption spectra, recorded with partial fluorescence yield, of polycrystalline $Fe_{1.01}Se$ for pressure varied in the range 0.5–65.6 GPa. The inset displays the crystal structure of $Fe_{1.01}Se$.

III. RESULTS AND DISCUSSION

Figure 1 shows Fe K-edge x-ray absorption spectra of polycrystalline $Fe_{1.01}Se$ recorded at P varied in the range 0.5–65.6 GPa. The spectra were obtained in partial fluorescence yield, with the spectrometer energy fixed at the maximum of the Fe $K\beta_{13}$ emission line (~7058 eV). At ambient pressure, the Fe K-edge absorption spectrum of tetragonal $Fe_{1.01}Se$ consists of a pre-edge peak A1 and two pronounced broad lines B and C on the side of greater photon energy. The general features of the Fe K-edge spectrum of tetragonal $Fe_{1.01}Se$ are similar to those of $LaFeAsO_{1-x}F_x$ samples.[30,31] Because the Fe atom in $Fe_{1.01}Se$ is in a tetrahedral site without a center of symmetry, the Fe $3d$ orbital is hybridized with Fe $4p$ orbitals. As the quadrupole transition Fe $1s \rightarrow 3d$ is very weak, the observed pronounced pre-edge peak A1 in Fe K-edge x-ray absorption spectra of $Fe_{1.01}Se$ in Fig. 1 predominantly originates from the dipole transition of a Fe $1s$ electron to unoccupied Fe $3d$-Se $4p$ hybrid bands.[32] Accordingly, a varying intensity of pre-edge peak A1 is thus an indicator of a varying local geometry or local distortion around the Fe atoms in $Fe_{1.01}Se$ under pressure. The high-energy features B and C are dominated by dipole transitions from the Fe $1s$ core electron to Fe $4p$ unoccupied states. Feature B, ~7120 eV, is ascribed to unoccupied Fe $4p$-Se $4d$ hybrid bands.[32] Feature D at greater energy is due mainly to the photoelectron multiple scattering of Fe atoms with their nearest neighbors.

The intensity of the pre-edge line A1 at energy of ~7112.7 eV decreases progressively with $P \leqslant \sim 10$ GPa, indicating a varying local distortion around Fe atoms and a suppression of the Fe $3d$-Se $4p$ hybridization.[32] A new prepeak A2 at energy of ~7113.7 eV develops for $P > 13$ GPa and attains its maximum intensity at $P \approx 40$ GPa, indicating

formation of a new phase and in agreement with previous XRD experiments under pressure reported in the literature.[8,9,11,13] After $P > 40$ GPa, the intensity of pre-edge peak A2 decreases slightly. Upon increasing pressure, a substantial decrease of absorption features B and C, particularly feature B, was observed, along with an energy shift. This upward shift of energy for absorption features B and C occurs because the bond lengths of both Fe-Fe and Fe-Se in $Fe_{1.01}Se$ decrease upon applying pressure.[9,13] The rising absorption edge of Fe K-edge spectra of $Fe_{1.01}Se$ gradually shifts toward greater energy with increasing applied pressure, probably associated with the charge transfer between Fe and Se due to the shrinking of the bond lengths of Fe-Se upon pressurization.

The inset in Fig. 1 displays the crystal structure of $Fe_{1.01}Se$. Based on XRD of $Fe_{1.01}Se$, the interlayer Se(1)–Se(2) distance along the c axis has greater compression than the intralayer Se(1)–Se(1) distance on applying $P \leqslant$ 8–12 GPa.[9,11,13] The separation between FeSe interlayers along the c axis in $Fe_{1.01}Se$ hence decreases greatly upon applying pressure. As reported by Margadonna *et al.*, the c axis contracts by 7.3% at 7.5 GPa, whereas the basal plane contracts by 3.3% at 7.5 GPa.[11] This indicates a larger distortion along the stacking direction of FeSe layers in the c axis relative to the basal plane. Besides, the larger Se-Fe-Se bond angle of $\sim 112^\circ$ in the $FeSe_4$ tetrahedra in $Fe_{1.01}Se$ slightly increases with increasing pressure, whereas the smaller Se-Fe-Se bond angle of $\sim 105^\circ$ decreases rapidly with $P \leqslant$ 8–12 GPa.[9,11] This indicates that the distortion of $FeSe_4$ tetrahedra in $Fe_{1.01}Se$ increases considerably away from regular tetrahedral shape with increasing pressure. Accordingly, relative to the $FeSe_4$ tetrahedra in $Fe_{1.01}Se$ without a center of symmetry at ambient pressure, the local structure of $FeSe_4$ unit becomes a relatively centrosymmetric character of the Fe site upon pressurization, consequently reducing the p-d hybridization. Based on polarized Fe K-edge x-ray absorption of $FeSe_x$ crystals, pre-edge peak A and feature B show a larger density of states of corresponding to unoccupied Fe 3d-Se 4p and Fe 4p-Se 4d hybrid bands, respectively, along the c axis.[33,34] The larger compression along the c axis, accompanied by an increased $FeSe_4$ tetrahedral distortion of $Fe_{1.01}Se$ upon pressurization, suppresses the Fe 3d-Se 4p and Fe 4p-Se 4d hybridization, particularly along the c axis, and consequently leads to a decreased intensity of pre-edge peak A and feature B.[35] T_c of $Fe_{1.01}Se$ increased to 34–37 K on applying $P \leqslant$ 5.5–9 GPa and then slowly decreased under P from 10 to 22 GPa.[7–11] The greater the suppression of Fe 3d-Se 4p hybridization upon pressurization, the higher the observed superconducting transition temperature.

With the FDMNES code,[36] we performed Fe K-edge x-ray absorption calculations on $Fe_{1.01}Se$ with different structural symmetries, based on the structural parameters at various pressures from the literature.[13] In the present XAS simulation, a muffin-tin (MT) full-multiple-scattering (FMS) approach with the real energy-dependent exchange Hedin-Lundqvist potential was applied with a cluster radius $R = 5$ Å. The FMS calculations were performed using the MT potential constructed from 10% overlapped MT spheres of the specified radii. The calculated spectra were broadened using the Seah-Dench formula.[36] Figure 2 shows the simulated Fe K-edge absorption spectra of $Fe_{1.01}Se$ with varied structural symmetries under pressure. The simulated Fe K-edge absorption spectrum

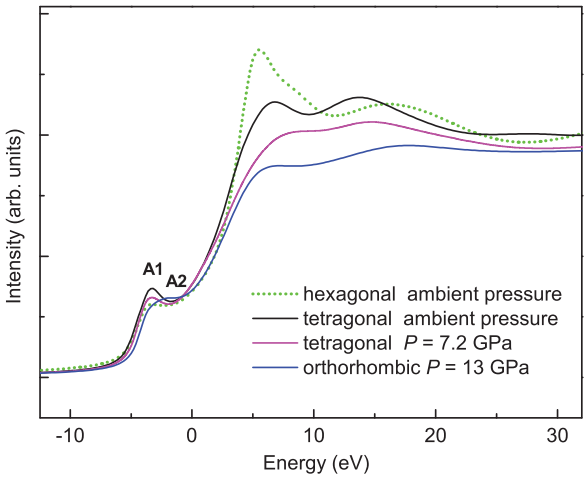

FIG. 2. (Color online) The simulated Fe K-edge absorption spectra of $Fe_{1.01}Se$ for the tetragonal, orthorhombic $Pbnm$, and hexagonal phases using the FDMNES code. The structural parameters of $Fe_{1.01}Se$ with different structural symmetries are based on the XRD refinements in the literature (Ref. 13).

of $Fe_{1.01}Se$ with tetragonal symmetry reproduces nicely with the overall profile of the Fe K-edge x-ray absorption spectrum of tetragonal phase $Fe_{1.01}Se$ at ambient pressure in Fig. 1. The pre-edge peak A1 is shifted to higher energy with increasing pressure, and a new pre-edge peak A2 develops for $P >$ 13 GPa, originating from a phase transition from the tetragonal structure to an orthorhombic symmetry. The experimental and calculated Fe K-edge spectra of $Fe_{1.01}Se$ agree satisfactorily.

In Fig. 3, the evolution of the Fe $K\beta$ x-ray emission line of $Fe_{1.01}Se$ as a function of $P \leqslant \sim$66 GPa is reproduced. The $K\beta$ emission spectra in Fig. 3 are normalized to the integrated area. The Fe $K\beta$ emission corresponds to a radiative decay of a Fe 1s core hole to a 3p level. As shown, the Fe $K\beta$ x-ray emission spectrum is divided into a main line $K\beta_{1,3}$ ($\sim$7058 eV) and a

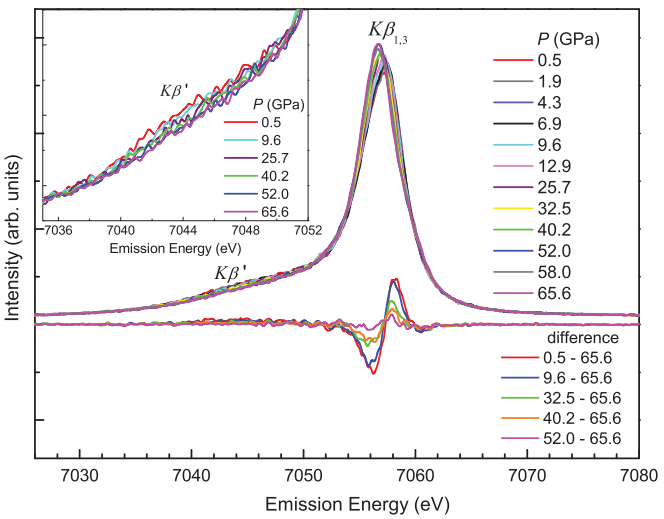

FIG. 3. (Color online) Evolution of the Fe $K\beta$ x-ray emission line of $Fe_{1.01}Se$ as a function of $P \leqslant \sim$66 GPa. At the bottom, intensity differences from the highest pressure emission spectrum (65.6 GPa) are shown for 0.5, 9.6, 32.5, 42.0, and 52.0 GPa. The inset displays the $K\beta$'□ satellite region for 0.5, 9.6, 25.7, 42.0, and 52.0 GPa.

satellite line $K\beta'$ (~7045 eV) due to the exchange interaction between the 3*p* core hole and the unfilled 3*d* shell in the final state of the emission. The energy separation between the satellite line $K\beta'$ and the main line $K\beta_{1,3}$ is proportional to the strength of the exchange interaction. The intensity of the satellite line $K\beta'$ is proportional to the net spin of the 3*d* shell and thus is indicative of the spin magnetic moment, as established by numerous studies on 3*d* transition-metal compounds.[37,38]

From Fig. 3, the Fe $K\beta$ emission line shape shows a considerable variation between 0.5 and 52 GPa, with the intensity of the satellite line $K\beta'$ progressively decreasing and the energy of main emission line $K\beta_{1,3}$ shifting to smaller emission energy. The position of the $K\beta_{1,3}$ line is shifted toward lower energy by ~0.6 eV with *P* increased to ~52 GPa. Above 52 GPa, the main line $K\beta_{1,3}$ for $Fe_{1.01}Se$ is narrower and more symmetric, with the intensity of the $K\beta'$ line and the position of the $K\beta_{1,3}$ line remaining nearly unchanged. The satellite line $K\beta'$ was gradually reduced in intensity upon applying pressure and became nearly absent for $P \approx 66$ GPa, indicating a continuous reduction of the spin moment of Fe in $Fe_{1.01}Se$ superconductors.

To extract the extent of the spin magnetic moment from the $K\beta$ emission spectra, several approaches have been applied, focusing on the variation of the $K\beta'$ satellite intensity or the full spectral shape or the $K\beta_{1,3}$ line position.[39–42] The integrated absolute value of the difference spectra is widely applied to deduce exactly the spin magnetic moment from the $K\beta$ emission spectrum.[38,41,43–45] The derived integrated absolute difference (IAD) values correlate linearly with the spin magnetic moment in the material. The procedures for analyzing the Fe $K\beta$ emission spectrum to obtain the IAD values involve normalizing the spectral area, shifting the spectra to the same center of mass, subtracting a reference spectrum (at 65.6 GPa, in this case) from all spectra, and integrating the absolute values of these difference spectra. We calculated the IAD value in the energy range of 7025–7070 eV.

Figure 4 shows the IAD values of Fe $K\beta$ emission spectra of $Fe_{1.01}Se$ as a function of applied pressure. The IAD values of the Fe $K\beta$ emission show a monotonic decrease for $P =$ 0.5–52 GPa, indicating a gradual decrease of spin magnetic moment of Fe^{2+} in $Fe_{1.01}Se$. The IAD values of the Fe $K\beta$ emission line decreased rapidly with $P \leqslant \sim 13$ GPa, decreased slowly after 13 GPa, and then remained nearly unchanged after 52 GPa. The discontinuous variation of the IAD values of the $K\beta$ emission line with varied declining slopes arises from a phase transition from a tetragonal structure to an orthorhombic structure for $P > 12$ GPa in $Fe_{1.01}Se$.[9,13]

Figure 5 shows Fe $K\beta$ emission spectra of $Fe_{1.01}Se$ with $P = 0.5$, 40.2, and 65.6 GPa and reference emission spectra of two iron-containing compounds with iron in the +2 oxidation state, FeS (high spin), and FeS_2 (low spin) at ambient pressure. The Fe $K\beta$ emission spectra in Fig. 5 were normalized, with the intensity of the main line $K\beta_{13}$ set to unity. The $K\beta'$ intensity of $Fe_{1.01}Se$ is notably less than that of FeS with the high-spin Fe^{2+} state. $Fe_{1.01}Se$ hence shows a small net magnetic moment of Fe^{2+} at ambient pressure, consistent with other measurements from neutron scattering and Mössbauer spectra for Fe-based superconductors.[16,46–49] The profile of the $K\beta'$ line for $Fe_{1.01}Se$

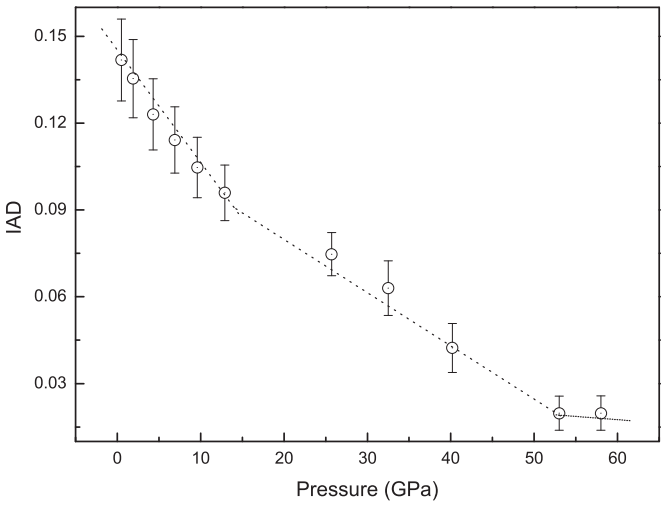

FIG. 4. IAD values of Fe $K\beta$ emission spectra of $Fe_{1.01}Se$ as a function of applied pressure. The dashed lines are for visual guidance.

at $P = 65.6$ GPa is almost coincident with that of FeS_2 with the low-spin Fe^{2+} state. This indicates that $Fe_{1.01}Se$ shows the low-spin state of Fe^{2+} ions upon applying $P \leqslant \sim 66$ GPa.

Based on spin-lattice relaxation in ^{77}Se NMR spectra for $Fe_{1.01}Se$, the Fe spins are collinearly AFM ordered.[22] For tetragonal β-FeSe, the Fe-Fe exchange coupling between nearest-neighbor (NN) spins is ferromagnetic (FM) and that between next-nearest-neighbor (NNN) spins is AFM, because Fe-Se-Fe angles relevant to their superexchange interactions are nearer 90° for the former and 180° for the latter.[16,50–52] Based on first-principles electronic structure calculations for β-FeSe, the NN FM superexchange interactions (J1) and NNN AFM superexchange interactions (J2) are J1 = 71 meV/Fe and J2 = 48 meV/Fe, respectively, at ambient pressure.[15] The increased $FeSe_4$ tetrahedral distortion away from a regular tetrahedra shape in $Fe_{1.01}Se$ upon pressurization reduces the Fe 3*d*-Se 4*p* hybridization, as evident in Fig. 1, and is expected to suppress the NN FM superexchange interactions mediated by Se4*p* orbitals.[15,50] The competition between the NN FM and

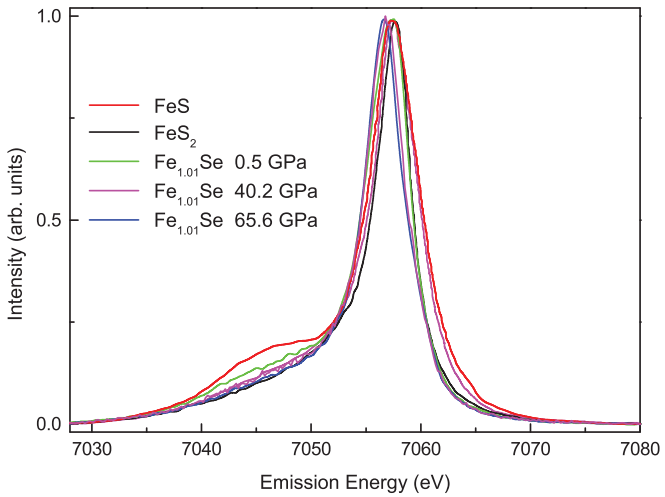

FIG. 5. (Color online) Fe $K\beta$ emission spectra of $Fe_{1.01}Se$ for $P = 0.5$, 40.2, and 65.6 GPa with reference emission spectra of FeS (high spin) and FeS_2 (low spin).

the NNN AFM superexchange interactions in $Fe_{1.01}Se$ upon pressurization accordingly enhances spin fluctuations.[22,50–52] A subtle balance of the competition between the NN FM and the NNN AFM superexchange interactions produces a collinear AFM spin arrangement in $Fe_{1.01}Se$.[15,16,22,50–52] The Fe-Fe spin fluctuations in $Fe_{1.01}Se$ thus decrease strongly the net magnetic moments of Fe ions, generating small net magnetic moments of Fe^{2+} at ambient pressure.[53]

IV. CONCLUSION

In this work, we presented comprehensive measurements of Fe K-edge XAS and Fe $K\beta$ XES of $Fe_{1.01}Se$ superconductors to probe the evolution of electronic structure and spin state under $P \leqslant \sim 66$ GPa. The intensity of the pre-edge line at energy of ~7112.7 eV in the Fe K-edge absorption spectra of $Fe_{1.01}Se$ decreases progressively with $P \leqslant \sim 10$ GPa. A new pre-edge line at energy of ~7113.7 eV develops for $P >$ 13 GPa, corresponding to a phase transition from the tetragonal to an orthorhombic symmetry (*Pbnm*) and in agreement with previous XRD experiments under pressure reported in the literature.[8,9,11,13] Comparison of pressure-dependent x-ray absorption spectra with FMS calculations using the FDMNES code shows satisfactory agreement between experimental and calculated Fe K-edge absorption spectra of $Fe_{1.01}Se$ under pressure. The larger compression along the c axis, accompanied by an increased $FeSe_4$ tetrahedral distortion of $Fe_{1.01}Se$ upon pressurization, decreases the Fe 3d-Se 4p and Fe 4p-Se 4d hybridization. Applied pressure suppresses the NN FM superexchange interaction mediated by Se 4p orbitals and enhances spin fluctuations on the Fe sites in $Fe_{1.01}Se$ through the competition between NN FM and NNN AFM superexchange interactions. The position of the $K\beta_{1,3}$ line is shifted toward lower energy by ~0.6 eV for pressure increased to ~66 GPa. The discontinuous variation of the IAD values of the $K\beta$ emission line was observed to originate from the phase transformation for $Fe_{1.01}Se > 12$ GPa. $Fe_{1.01}Se$ shows a small net magnetic moment of Fe^{2+} at ambient pressure, probably arising from strong Fe-Fe spin fluctuations. Based on the analysis by IAD methods, the variations of $K\beta'$ peak intensity and consequently the reduction of the net spin moment of Fe in $Fe_{1.01}Se$ upon applying pressure show a continuous change. $Fe_{1.01}Se$ shows the low-spin state of Fe^{2+} ions upon applying $P \leqslant \sim 66$ GPa. The experimental results provide insight into the Fe-Fe spin fluctuations and spin state of $Fe_{1.01}Se$ superconductors.

ACKNOWLEDGMENT

We thank the NSRRC staff for their technical support. This research is supported by the NSRRC and the National Science Council of the Republic of China under Grant No. NSC 99 2113-M-213-006.

*jmchen@nsrrc.org.tw

[1] Y. Kamihara, T. Watanabe, M. Hirano, and H. Hosono, J. Am. Chem. Soc. **130**, 3296 (2008).
[2] H. Takahashi, K. Igawa, K. Arii, Y. Kamihara, M. Hirano, and H. Hosono, Nature **453**, 376 (2008).
[3] H.-H. Wen, G. Mu, L. Fang, H. Yang, and X. Zhu, Europhys. Lett. **82**, 17009 (2008).
[4] T. Y. Chen, Z. Tesanovic, R. H. Liu, X. H. Chen, and C. L. Chien, Nature **453**, 1224 (2008).
[5] X. H. Chen, T. Wu, G. Wu, R. H. Liu, H. Chen, and D. F. Fang, Nature (London) **453**, 761 (2008).
[6] F. C. Hsu, J. Y. Luo, K. W. The, T. K. Chen, T. W. Huang, P. M. Wu, Y. C. Lee, Y. L. Huang, Y. Y. Chu, D. C. Yan, and M. K. Wu, Proc. Nat. Acad. Sci. USA **105**, 14262 (2008).
[7] Y. Mizuguchi, F. Tomioka, S. Tsuda, T. Yamaguchi, and Y. Takano, Appl. Phys. Lett. **93**, 152505 (2008).
[8] S. Medvedev, T. M. McQueen, I. A. Troyan, T. Palasyuk, M. I. Eremets, R. J. Cava, S. Naghavi, F. Casper, V. Ksenofontov, G. Wortmann, and C. Felser, Nat. Mater. **8**, 630 (2009).
[9] G. Garbarino, A. Sow, P. Lejay, A. Sulpice, P. Toulemonde, M. Mezouar, and M. Núñez-Regueiro, Europhys. Lett. **86**, 27001 (2009).
[10] D. Braithwaite, B. Salce, G. Lapertot, F. Bourdarot, C. Marin, D. Aoki, and M. Hanfland, J. Phys. Condens. Matter **21**, 232202 (2009).
[11] S. Margadonna, Y. Takabayashi, Y. Ohishi, Y. Mizuguchi, Y. Takano, T. Kagayama, T. Nakagawa, M. Takata, and K. Prassides, Phys. Rev. B **80**, 064506 (2009).
[12] O. Tkachenko, A. Morawski, A. J. Zaleski, P. Przyslupski, T. Dietl, R. Diduszko, A. Presz, and K. Werner-Malento, J. Supercond. Nov. Magn. **22**, 599 (2009).
[13] R. S. Kumar, Y. Zhang, S. Sinogeikin, Y. Xiao, S. Kumar, P. Chow, A. L. Cornelius, and C. Chen, J. Phys. Chem. B **114**, 12597 (2010).
[14] M. D. Lumsden and A. D. Christianson, J. Phys. Condens. Matter **22**, 203203 (2010).
[15] F. Ma, W. Ji, J. Hu, Z.-Y. Lu, and T. Xiang, Phys. Rev. Lett. **102**, 177003 (2009).
[16] A. Kumar, P. Kumar, U. V. Waghmare, and A. K. Sood, J. Phys. Condens. Matter **22**, 385701 (2010).
[17] E. Z. Kurmaev, R. G. Wilks, A. Moewes, N. A. Skorikov, Yu. A. Izyumov, L. D. Finkelstein, R. H. Li, and X. H. Chen, Phys. Rev. B **78**, 220503 (2008).
[18] C.-Y. Moon and H. J. Choi, Phys. Rev. Lett. **104**, 057003 (2010).
[19] A. Subedi, L. Zhang, D. J. Singh, and M. H. Du, Phys. Rev. B **78**, 134514 (2009).
[20] J. Zhao, Q. Huang, C. de la Cruz, S. Li, J. W. Lynn, Y. Chen, M. A. Green, G. F. Chen, G. Li, Z. Li, J. L. Luo, N. L. Wang, and P. Dai, Nat. Mater. **7**, 953 (2008).
[21] T. M. McQueen, M. Regulacio, A. J. Williams, Q. Huang, J. W. Lynn, Y. S. Hor, D. V. West, M. A. Green, and R. J. Cava, Phys. Rev. B **78**, 024521 (2008).
[22] T. Imai, K. Ahilan, F. L. Ning, T. M. McQueen, and R. J. Cava, Phys. Rev. Lett. **102**, 177005 (2009).
[23] T. Yildirim, Phys. Rev. Lett. **101**, 057010 (2008).
[24] K.-W. Lee, V. Pardo, and W. E. Pickett, Phys. Rev. B **78**, 174502 (2008).

[25]R. A. Jishi and H. M. Alyahyaei, New J. Phys. **11**, 083030 (2009).
[26]J. M. Chen, T. L. Chou, J. M. Lee, S. A. Chen, T. S. Chan, C. K. Chen, K. T. Lu, H.-S. Sheu, C. M. Lin, N. Hiraoka, H. Ishii, and T. J. Yang,, Phys. Rev. B **79**, 165110 (2009).
[27]F. Bridges, C. H. Booth, M. Anderson, G. H. Kwei, J. J. Neumeier, J. Snyder, J. Mitchell, J. S. Gardner, and E. Brosha, Phys. Rev. B **63**, 214405 (2001).
[28]J.-P. Rueff, L. Journel, P.-E. Petit, and F. Farges, Phys. Rev. B **69**, 235107 (2004).
[29]J.-P. Rueff, C.-C. Kao, V. V. Struzhkin, J. Badro, J. Shu, R. J. Hemley, and H. K. Mao, Phys. Rev. Lett. **82**, 3284 (1999).
[30]N. Kaurav, Y. T. Chung, Y. K. Kuo, R. S. Liu, T. S. Chan, J. M. Chen, J.-F. Lee, H.-S. Sheu, X. L. Wang, S. X. Dou, S. I. Lee, Y. G. Shi, A. A. Belik, K. Yamaura, and E. Takayama-Muromachi, Appl. Phys. Lett. **94**, 192507 (2009).
[31]A. Ignatov, C. L. Zhang, M. Vannucci, M. Croft, T. A. Tyson, D. Kwok, Z. Qin, and S.-W. Cheong e-print arXiv:0808.2134 (unpublished).
[32]F. de Groot, G. Vankó, and P. Glatzel, J. Phys. Condens. Matter **21**, 104207 (2009).
[33]B. Joseph, A. Iadecola, L. Simonelli, Y. Mizuguchi, Y. Takano, T. Mizokawa, and N. L. Saini, J. Phys. Condens. Matter **22**, 485702 (2010).
[34]B. C. Chang, Y. B. You, T. J. Shiu, M. F. Tai, H. C. Ku, Y. Y. Hsu, L. Y. Jang, J. F. Lee, Z. Wei, K. Q. Ruan, and X. G. Li, Phys. Rev. B **80**, 165108 (2009).
[35]H. Yamaoka, I. Jarrige, A. Ikeda-Ohno, S. Tsutsui, J.-F. Lin, N. Takeshita, K. Miyazawa, A. Iyo, H. Kito, H. Eisaki, N. Hiraoka, H. Ishii, and K.-D. Tsuei, Phys. Rev. B **82**, 125123 (2010).
[36]Y. Joly, Phys. Rev. B **63**, 125120 (2001).
[37]H. Yamaoka, N. Tsujii, H. Oohashi, D. Nomoto, I. Jarrige, K. Takahiro, K. Ozaki, K. Kawatsura, and Y. Takahashi, Phys. Rev. B **77**, 115201 (2008).
[38]A. Mattila, T. Pylkkänen, J.-P. Rueff, S. Huotari, G. Vankó, M. Hanfland, M. Lehtinen, and K. Hämäläinen, J. Phys. Condens. Matter **19**, 386206 (2007).
[39]J. P. Rueff, M. Krisch, Y. Q. Cai, A. Kaprolat, M. Hanfland, M. Lorenzen, C. Masciovecchio, R. Verbeni, and F. Sette, Phys. Rev. B **60**, 14510 (1999).
[40]J. Badro, J.-P. Rueff, G. Vankó, G. Monaco, G. Fiquet, and F. Guyot, Science **305**, 383 (2004).
[41]J.-P. Rueff, A. Shukla, A. Kaprolat, M. Krisch, M. Lorenzen, F. Sette, and R. Verbeni, Phys. Rev. B **63**, 132409 (2001).
[42]P. Glatzel and U. Bergmann, Coord. Chem. Rev. **249**, 65 (2005).
[43]G. Vankó, T. Neisius, G. Molnár, F. Renz, S. Kárpáti, A. Shukla, and F. M. F. de Groot, J. Phys. Chem. B **110**, 11647 (2006).
[44]G. Vankó, J.-P. Rueff, A. Mattila, Z. Németh, and A. Shukla, Phys. Rev. B **73**, 024424 (2006).
[45]R. Lengsdorf, J.-P. Rueff, G. Vankó, T. Lorenz, L. H. Tjeng, and M. M. Abd-Elmeguid, Phys. Rev. B **75**, 180401 (2007).
[46]Y. Qiu, W. Bao, Q. Huang, T. Yildirim, J. M. Simmons, M. A. Green, J. W. Lynn, Y. C. Gasparovic, J. Li, T. Wu, G. Wu, and X. H. Chen, Phys. Rev. Lett. **101**, 257002 (2008).
[47]C. de la Cruz, Q. Huang, J. W. Lynn, J. Li, W. Ratcliff II, J. L. Zarestky, H. A. Mook, G. F. Chen, J. L. Luo, N. L. Wang, and P. Dai, Nature **453**, 899 (2008).
[48]A. Błachowski, K. Ruebenbauer, J. Żukrowski, J. Przewoźnik, K. Wojciechowski, and Z. M. Stadnik, J. Alloys Compd. **494**, 1 (2010).
[49]Q. Huang, Y. Qiu, W. Bao, M. A. Green, J. W. Lynn, Y. C. Gasparovic, T. Wu, G. Wu, and X. H. Chen, Phys. Rev. Lett. **101**, 257003 (2008).
[50]Q. Si and E. Abrahams, Phys. Rev. Lett. **101**, 076401 (2008).
[51]P. Kumar, A. Kumar, S. Saha, D. V. S. Muthu, J. Prakash, S. Patnaik, U. V. Waghmare, A. K. Ganguli, and A. K. Sood, Solid State Comm. **150**, 557 (2010).
[52]D.-X. Yao and E. W. Carlson, Phys. Rev. B **78**, 052507 (2008).
[53]Z.-Y. Lu, F. Ma, and T. Xiang, J. Phys. Chem. Solids, **72**, 319 (2011).